Structure and reactivity of TNT and related species: Application of spectroscopic approaches and quantum–chemical approximations toward understanding transformation mechanisms

Mohammad Qasim [a,*], Leonid Gorb [b], David Magers [c], P. Honea [d], J. Leszczynski [a,e], Brett Moore [a,c], Lyssa Taylor [a,c], Matthew Middleton [a,f]

[a] USACE ERDC-EL, 3909 Halls Ferry Road, Vicksburg, MS 39180, United States
[b] SpecPro, 3909 Halls Ferry Road, Vicksburg, MS 39180, United States
[c] Mississippi College, 2000 South Capital Street, Clinton, MS 39058, United States
[d] University of Mississippi School of Medicine, 2500 North State Street, Jackson, MS 39216, United States
[e] Computational Center for Molecular Structure and Interactions, Jackson State University, 1400 Lynch Street, Jackson, MS 39217, United States
[f] Mississippi State University, Mississippi State, Starkville, MS 39762, United States

ARTICLE INFO

ABSTRACT

This paper presents our latest findings regarding the structure and reactivity of the nitroaromatics, TNT and selected derivatives, within their environmental context. We also demonstrate the useful and proactive role of combined computational chemistry and spectroscopy tools in studying competing transformation mechanisms, particularly those with toxic potential.

TNT and selected derivatives were reacted via alkaline hydrolysis as well as via free radical initiators through monochromatic irradiation and through Fenton reactions in complex competing transformation mechanisms. Only alkaline hydrolysis produced consistent and effective transformation intermediate and final products in this research. However, irradiation of the product generated by alkaline hydrolysis at 450 nm (wavelength of maximum absorption) caused complete disappearance of the spectra.

Published by Elsevier B.V.

1. Introduction

TNT is well known for its widespread presence and toxicity in the environment. At documented concentrations, TNT is considered highly toxic, mutagenic, and potentially carcinogenic [1–3]. Environmental accumulation increases the chance of human contact. Problems ranging from high cost to incomplete and slow mineralization, toxic intermediates, and unstable treatment cultures have plagued physico-chemical, biological, and biochemical attempts at degradation of TNT and its derivatives [4–17]. However, the ever-increasing and cost-effective use of computational chemistry (CC) to predict appropriate transformation mechanisms has yielded potentially acceptable intermediate and final products [18]. In addition, CC methods are essential to the analysis of hazardous or inaccessible "parent" compounds and their transformations as well as effective in the study of molecular interactions with the environment. Computational methods combined with spectroscopic techniques have proven useful in finding chemically feasible transformation products [19–20,28,33]. Goals have been to discover hypotheses, methodology and data to build a system of knowledge useful to understanding the transformation mechanisms of compounds of interest to the DoD and chemical industries. This research is part of an ongoing investigation of nitroaromatic energetics and focuses on TNT and selected transformation products.

Theoretical calculation plus selective spectroscopic verification provided a valid approach to the premise that *molecular structure determines transformation pathways*. It is expected that this combination of methods, based on computational simulation plus selective spectroscopic verification, has the potential to provide a powerful research tool for developing effective, in-situ cleanup technologies for explosives and other contaminant materials.
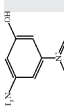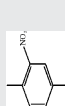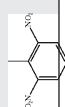
Methodology for this study began with semiempirical CC prediction of TNT and its derivatives being carried out to ascertain physical structure and chemical properties. Second, much of our data was then verified spectroscopically to ensure chemical feasibility of the transformation products and mechanisms. This experimental aspect included application of alkaline hydrolysis (Section 4.2) and methods of producing free radicals (via monochromatic irradiation and Fenton reagents (Section 4.5). Last, Density Functional Theory

Table 1
Energies and other properties of TNT and other compounds.

Compound		MM2 total steric energy (kcal/mol)	Orbital level	B3LYP			AM1 minimal energy			
				HOMO/LUMO energies (eV)		Heat of formation (kcal/mol)	HOMO/LUMO energies (eV)		Heat of formation (kcal/mol)	Dipole charge (debye)
Energies and some properties of TNT and related compounds										
2,4,6-Trinitrotoluene		6.4610	N = 43 N = 42	LUMO HOMO	−0.13410 −0.31784	17.112	LUMO HOMO	−2.43 −11.72	42.259	0.941
2-Amino-4,6-dinitrotoluene		−0.8787	N = 38 N = 37	LUMO HOMO	−0.10816 −0.25269	11.106	LUMO HOMO	−1.63 −9.53	28.579	7.191
4-Amino-2,6-dinitrotoluene		−0.2180	N = 38 N = 37	LUMO HOMO	−0.10493 −0.24772	14.878	LUMO HOMO	−1.65 −9.45	31.087	5.459
2,6-Diamino-4-nitrotoluene		−4.9658	N = 33 N = 32	LUMO HOMO	−0.08143 −0.21899	10.370	LUMO HOMO	−0.66 −8.58	18.968	7.116
2,4-Diamino-6-nitrotoluene		−4.8493	N = 33 N = 32	LUMO HOMO	−0.07746 −0.21269	13.676	LUMO HOMO	−0.62 −8.41	20.823	6.766
2,4,6-Triaminotoluene		−9.0304	N = 28 N = 27	LUMO HOMO	0.02846 −0.18403	17.562	LUMO HOMO	1.31 −7.66	15.490	0.094
2,4,6-Trinitrophenol		3.9152	N = 43 N = 42	LUMO HOMO	−0.14893 −0.30900	−23.797	LUMO HOMO	−2.53 −11.41	0.939	1.53
2-Amino-4,6-dinitrophenol		2.5323	N = 38 N = 37	LUMO HOMO	−0.12048 −0.24461	−33.552	LUMO HOMO	−1.73 −9.38	−12.485	6.017
4-Amino-2,6-dinitrophenol		−5.6038	N = 38 N = 37	LUMO HOMO	−0.12335 −0.24039	−23.599	LUMO HOMO	−1.87 −9.31	−8.378	6.142
2-Hydroxy-4,6-dinitrotoluene		−3.1551	N = 38 N = 37	LUMO HOMO	−0.11512 −0.27606	−31.936	LUMO HOMO	−1.95 −10.47	−13.646	5.397
4-Hydroxy-2,6-dinitrotoluene		−8.1751	N = 38 N = 37	LUMO HOMO	−0.11212 −0.27248	−27.052	LUMO HOMO	−1.86 −10.37	−11.786	3.539
2,6-Dihydroxy-6-nitrotoluene		−4.9939	N = 33 N = 32	LUMO HOMO	−0.09423 −0.24887	−78.082	LUMO HOMO	−1.20 −9.69	−66.280	7.223
2,4-Di hydroxy-6-nitrotoluene		−2.1985	N = 33 N = 32	LUMO HOMO	−0.08960 −0.24033	−73.676	LUMO HOMO	−1.19 −9.56	−65.168	4.836
1,3,5-Trinitrobenzene		3.2040	N = 40 N = 39	LUMO HOMO	−0.14149 −0.33665	19.386	LUMO HOMO	−2.68 −12.75	44.662	0.002
5-Amino-1,3-dinitrobenzene		−6.3134	N = 35 N = 34	LUMO HOMO	−0.11424 −0.25560	15.581	LUMO HOMO	−1.71 −9.67	32.294	6.748

Compound											
5-Amino-1-hydroxy-3-nitrobenzene	−5.7349	N = 30 / N = 29	LUMO / HOMO	−26.639	LUMO / HOMO	−0.09051 / −0.23030	LUMO / HOMO	−0.93 / −9.04	LUMO / HOMO	−18.748	7.26
2,4-Di nitrotoluene	−2.2109	N = 35 / N = 34	LUMO / HOMO	10.118	LUMO / HOMO	−0.11546 / −0.30488	LUMO / HOMO	−1.85 / −11.03	LUMO / HOMO	28.291	5.655
2,6-Dinitrotoluene	2.3992	N = 35 / N = 34	LUMO / HOMO	15.027	LUMO / HOMO	−0.11119 / −0.29770	LUMO / HOMO	−1.82 / −10.95	LUMO / HOMO	31.201	3.508

The compounds listed comprise degradation products of nitroaromatic explosives that could be found in contaminated soils. Structural strains were minimized with MM2. AM1 semiempirical methods were employed to calculate HOMO/LUMO energies, heats of formation, and dipole charges. B3LYP was used to verify the AM1 HOMO/LUMO and heat of formation energy calculations.

(DFT) calculations were performed at the B3LYP (Beck 3 Parameter, Lee, Yang, Parr) level to support and expand our investigation of TNT and selected species (Table 1 and [20,33]).

Since *molecular structure determines transformation pathways*, a section on TNT molecular structure (Section 3) was added to facilitate understanding of this study's results and conclusions.

2. Theoretical and spectroscopic approaches

2.1. Computational methods

Computational chemistry is based on simulation. Our study utilized various levels of CC, including semiempirical and DFT methods for prediction of molecular structures; modes and sites of reactivity; as well as rates of transition state formation, fast-forming intermediate and final products—all of which contributed to revealing the reaction mechanisms of the competing transformation pathways of TNT and seventeen analogues.

*M*olecular *O*rbital *PAC*kage (MOPAC) is fast and uses comparatively less memory than most CC tools. Since TNT and its analogues have similar structures/similar entropies, MOPAC provided data sufficiently accurate to compare the important physical and chemical properties: structure; electronic distribution; dipole moments; and thermodynamics (heats of formation). Utilizing classical mechanics, MOPAC *M*olecular *M*echanics (MM2 and MM3) predicted such properties as steric hindrance (used for geometrical optimization and distinguishing stabilities of molecular conformers), while quantum mechanical semiempirical methods calculated bond lengths and angles, molecular orbitals, dihedral angles, formation and steric energies, partial charges, electrostatic potentials, dipole charges/dipole moments, cosmo solvation, solvent accessibility surfaces, and HOMO/LUMO energy values. Definite trends were revealed (and are discussed in Section 5) corresponding to substituent nature, position, and number of amino and hydroxyl groups ([19–20,33] and Table 1). HOMO/LUMO energies reveal aspects of molecular structure and can thereby indicate potential toxicity and recalcitrance (Section 5).

DFT calculations were run at the B3LYP/6-311G(d,p) level via the use of homodesmotic reactions. Although DFT B3LYP level 3 values are higher than those obtained through MOPAC methods, the DFT predictions from the study corroborate similar trends (Section 4.2) to those obtained via AM1 (Table 1).

2.2. Spectroscopic approach/instrumentation

Theoretical results as to fast-forming states, intermediate and final products were supported and verified via UV Vis, and Stopped Flow (SF) spectroscopy. A Genesys 2 UV Vis Spectrophotometer was used in conjunction with 10 mm pathlength quartz cuvettes. Measurements were taken from 200 to 700 nm. UV Vis (Figs. 1 and 2A–C) was used to measure concentrations and to follow courses of chemical reactions through changes in shape and wavelength (Section 4.2). Concentration measurements of parent, intermediate and final compounds were observed through changes in height of their spectra where maximum absorption occurs. Changes in spectral shape (appearance/disappearance of shoulders; site of wavelengths of maximum absorption) indicated the appearance and disappearance of intermediate and final transformations.

A Hi-Tech SF-61 Stopped Flow Spectrophotometer was used to measure rate constants and to follow rates of fast-forming intermediates (Fig. 3A–F), indicating steps of the reactions through changes in slope (Section 4.2). This technique is theoretically capable of following rates as small as a thousandth of a second.

A monochromatic irradiation system designed for performing photochemical reactions was constructed and used to carry out

photochemically induced free radical reactions at wavelengths of maximum absorption. This system uses a 200 W Hg (Xe) lamp housed in a compartment with mirrors and focusing lenses. It is equipped with a sample holder which accommodates standard 3 mL quartz cuvettes, a beam splitter, and three monochromators. One monochromator is placed perpendicular to the incident light; one is a scanning monochromator that detects absorbed light passed through the sample; and the third, perpendicular to the sample, measures emissions. These monochromators can be set manually for samples to be irradiated at their wavelength of maximum absorbance. The amount of energy is read directly with multifunctional meters with phototube detection systems. This irradiation system is also capable of measuring absorbance and emission quantum yields, revealing changes in excited states and, thereby, competing mechanisms. Section 4.5 discusses TNT and product irradiation. A study of quantum yields of photochemical reactions of nitroaromatic energetics will be carried out in the future.

2.3. Spectroscopic approach/procedure

Serial dilutions of varied concentrations of reagent grade sodium hydroxide (NaOH) were added to fixed concentrations of TNT. TNT with no NaOH was used as a standard for comparison. Fenton reagents of hydrogen peroxide (H_2O_2) and ferrous perchlorate ($Fe(ClO_4)_2$) at appropriate concentrations were made immediately prior to obtaining spectra. These concentrations and accompanying reactions are discussed in Sections 4.2 and 4.5 and are shown in Fig. 7. All experiments were repeated three times under the same experimental conditions to verify reproducibility.

3. TNT molecular structure

TNT exists in two known crystallographic forms: monoclinic and orthorhombic in which the TNT nitro groups adopt a non-planar configuration due to crystal packing forces, extensive inter- and intramolecular van der Waals interactions, and to steric effects of the methyl group [33]. Recent *ab initio* Hartree-Fock and DFT calculations appear to account for the steric effects of the methyl group, with the 2- and 6-nitro groups predicted to be non-planar and the 4-nitro group planar to the phenyl ring [19–20]. TNT carbon rings are planar and aromatic with equal angles of 120° [19–20,23–27]. The aromaticity of TNT is due to its planar π system distribution, including that of its nitro groups.

The π-system of TNT is electron-deficient due to its planar aromatic structure, where π-electrons are drawn away from the ring and towards the electron-withdrawing nitro groups via resonance. TNT electron deficiency and planarity facilitate complexation with the non-bonding (n) electrons of a donating group, such as the oxygen atoms in a co-planar medium [28–29]. These TNT properties lessen its dissolution and, therefore, its mobility and transport in the environment. However, substitution at TNT ortho positions by such electron-donating groups as methyl, amino, and hydroxide ions (OH⁻) can lessen the electron deficiency of the π system and prevent co-planarity with electron-donating groups from the media—minimizing complexation and increasing dissolution [19–20,23–27], thereby, affecting risk to the environment. Increased solubility escalates dispersal, including that of such toxic substances as TNT.

4. TNT reactivity

4.1. Four effects and general reactivity

Four major effects govern chemical reactivity of nitro groups in TNT and related molecules: resonance, inductive, steric hin-

drance, and intramolecular electrostatic interaction between the nitro group oxygen atoms and atoms of the methyl group (or in TNT derivatives, such electron-donating substituents as amine or hydroxyl groups). TNT nitro groups 2 and 6 are adjacent to the methyl group and are most subject to these four effects [19–20,23–27]. These nitro groups are most sterically hindered by the methyl group, which inductively provides them with electrons.

Data from this study, obtained via semiempirical and DFT B3LYP methods, confirmed that the position of the nitro groups is sensitive to the influence of substituents placed in the ortho position; selected molecular configurations obtained via DFT further illustrate this point [19–20]. This importance of substituent position on the aromatic ring to its reactivities was supported spectroscopically as shown in Table 1.

Due to resonance stabilization by which the π-electrons are drawn away by resonance from all positions toward the nitro group outside the ring, nitro groups in nitroaromatic compounds deactivated all positions on the ring, with carbons ortho and para to the carbon having the nitro groups becoming the most deactivated [23–27,30]. Deactivation of the carbons ortho and para to the nitro group rendered them susceptible to nucleophilic attack by OH⁻. This mechanism competes with the Meisenheimer complex in which the OH⁻ attacks the carbon having the nitro group, causing brief formation of a transition state in which both nucleophile and nitro group are still attached to the same carbon before elimination of the nitro group [4–5,19–20].

According to the results of our calculations and textbook chemistry, nitro groups are theoretically good leaving groups in nucleophilic reactions [19–20,23–27]. The presence of an OH⁻ instead of the methyl group lowered steric hindrance sufficiently to facilitate nitro group removal. These electrostatic interactions between the hydrogen atoms of the methyl group and the oxygen atoms of the ortho 2- and 6-nitro groups prevented effective chemical transformations of TNT to DNT by electrophilic attack on the carbon bonded to the electron-withdrawing nitro groups. Thus, nucleophilic rather than electrophilic substitutions are preferred for TNT chemical transformation [4–5,19–20]. In addition, nucleophilic transformations result in formation of more easily biodegraded hydroxylated nitro compounds, particularly when the two hydroxyl groups are ortho or para to each other [19–20].

4.2. Alkaline hydrolysis

Sodium hydroxide (NaOH) acted as a hydrolyzing agent in separate sets of experiments [4–5,19–20] with the expectation that complete degradation would result from the loss of aromaticity. TNT was chemically transformed into TNP and other competing products with high biodegradability via nucleophilic reactions, thereby initiating complex competing reactions in which time and nucleophilic concentration influenced production of mono- and di-hydroxylated aromatic intermediates [4–5,19–20].

Electron donor–acceptor interactions result in TNT reacting with soil and other natural organic materials in the environment, thus influencing its mobility, bioavailability, and reactivity—all of which have potential to impinge on toxicity levels [31]. Experimental data for alkaline hydrolysis of TNT in aqueous solutions, suggesting that alkali transformation of TNT takes place through formation of color-producing intermediates that are further transformed to non-aromatic compounds, were reported at pH 12 [4–5]. Fig. 2 presents UV Vis spectra of 50 ppm TNT + 0.05N NaOH (A); 50 ppm TNT + 0.5N NaOH (B); and 50 ppm TNT + 1.0N NaOH (C). The UV Vis spectra showed a rapid decrease in the 235 nm band (abs_{max}) and also development of absorbance bands at 250 and 450 nm with increasing OH⁻ concentrations. This reaction at pH 12 was quite fast with 25 ppm TNT being transformed into non-aromatic compounds within 6 h.
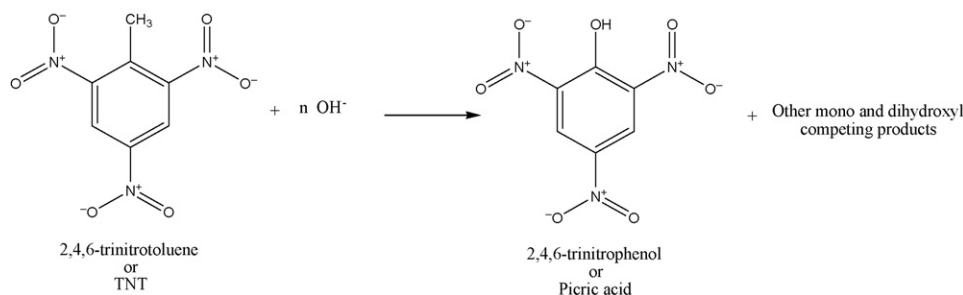
Fig. 1. TNT oxidation to TNP. TNT is the final oxidation step in the transformation of TNT when reacted with hydroxide ion. The methyl group is oxidized. Other products are also formed in the alkaline hydrolysis of TNT.

Stopped Flow spectra were taken to measure rates of TNT disappearance as well as the appearance of an intermediate product, corroborating findings revealed by UV Vis spectra as to TNT absorbance/disappearance at the 235 nm band. The intermediate product appearance at 450 nm basically mirrors this disappearance in A–B and in C–D of Fig. 3. Fig. 3 compares SF spectra of 50 mg/L TNT at 235 nm (A and C), to SF spectra at 450 nm (B and D). The K constant scale for A–B is 30 s and that for C–D is log based to 1000 s. Upon increases in NaOH concentration between 0.05N and 1.0N of NaOH, SF spectra clearly demonstrate increasingly rapid disappearance of TNT absorbance at 235 nm. At 1.0N, high concentration, a different mechanism appeared to be operative during only the initial three seconds of reaction time. This might possibly indicate a product resulting from dimerization and remains to be investigated (Section 4.4).

Significant amounts of nitrite were released, indicating that the resultant compounds from TNT alkaline hydrolysis are not only non-aromatic, but also less nitrated [4]. However, the presence of nitro groups in these non-aromatic compounds is not considered a drawback in light of the easy-leaving character of nitro groups. Thus, oxidative attack on the exposed carbon backbone may even be enhanced by the electron-withdrawing nature of the nitro groups [19–20].

4.3. Reduction

Although this was not bioenvironmental research, reductive principles are necessary to understanding TNT transformation. Effective reductive transformations of TNT occur through bioreductive systems that generate amine derivatives. Transformation can also occur chemically via hydride ions [5,17]. Fig. 4 shows the TNT reductive transformation mechanisms to nitroaromatic amines of both bio- and hydride reduction. The three steps depicted are the formation of nitroso derivatives, followed by hydroxyl amines and, finally, by the formation of amine derivatives.

4.4. Polymerization

Polymerization was not studied per se. However, stoichiometric explanations do not account for the amount of TNT after reactions have taken place. In addition, polymerization reactions constitute another competing mechanism that can occur at high alkaline concentrations on various sites on the TNT molecule. For example, upon loss of a proton from the methyl group carbon (proton abstraction resulting from high concentration of base), one TNT molecule can act as a nucleophile for another TNT molecule by attacking its positively charged atoms, thus forming a dimer [32].
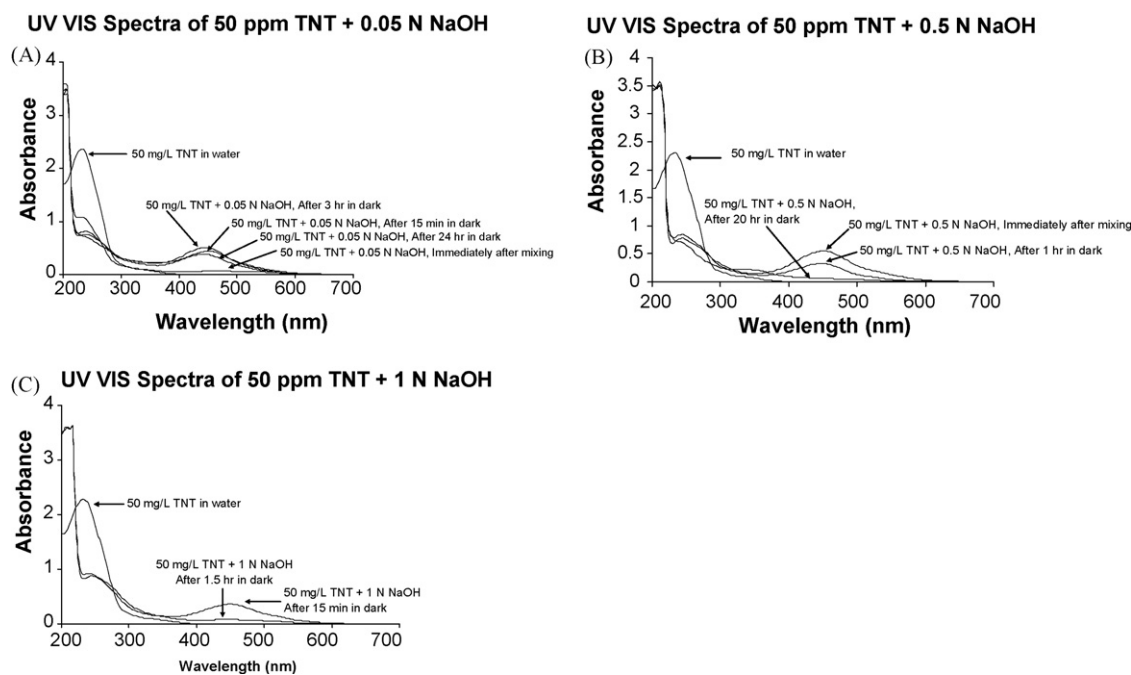

Fig. 2. UV Vis spectra of TNT after treatment with sodium hydroxide. 50 ppm TNT is treated with (A) 0.05N NaOH; (B) 0.5N NaOH; and (C) 1N NaOH; and UV Vis spectra were collected at intervals over a 24 h time period. A through C shows the progression of a higher rate of transformation dependent on increased concentration and length of time.
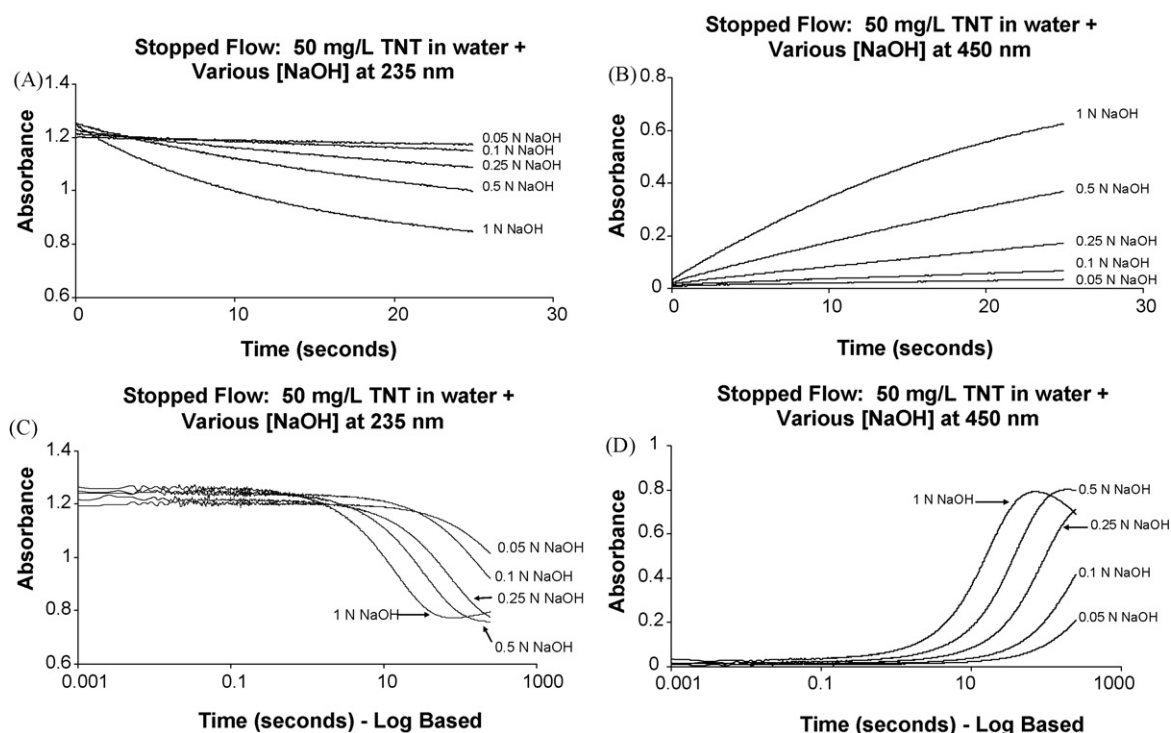
Fig. 3. Stopped Flow of TNT after treatment with sodium hydroxide. Stopped Flow spectra of 50 ppm TNT were taken at 235 nm (A and C) and compared to SF data taken at 450 nm (B and D). Data were taken after 30 s for (A) and (B). (C and D) data were log base extrapolated to 1000 s. Initially, TNT has a maximum peak at 235 nm. Degradation of this peak was followed via SF after reaction with NaOH. New peak formation occurred at 450 nm and was also followed via SF.

Dimerization can also occur at different TNT molecular sites, such as between nitrogen atoms of two molecules or between one nitrogen atom from one molecule and a carbon from another [23–26,32].

Polymerization can result in the creation of toxic compounds. Some di-azo polymers of TNT can be expected to be highly toxic, similar to the toxicity of azo dyes. Also, in regard to toxicity, OH^- groups render molecules to which they are attached more water soluble, thereby facilitating metabolism. For example, adding two adjacent OH^- to benzene causes benzene to become sufficiently soluble to be metabolized by humans. Under certain conditions, the two adjacent OH^- lose a water molecule and form an epoxy, which is the cause of benzene's carcinogenicity. Due to its molecular structure, the same principles regarding OH^- contributing to solubility and to the occasional formation of an apoxy (due to loss of a water molecule) are applicable to TNT [13,32].

4.5. Free radical reactions via photolysis and Fenton reagents

TNT was introduced into a specially designed and constructed monochromatic irradiation system, which oxidized TNT via the OH radical (Fig. 5). Results of irradiation showed the formation of 1,3,5-trinitrobenzene (TNB) due to an oxidation mechanism, which is more light dependent than the reduction mechanism responsible for the formation of the other nitroaromatic amines. UV Vis data suggest that photolysis did not provide a means of degradation for TNT at its maximum absorption wavelength, 235 nm; this lack of transformation is reflected by UV Vis spectra of 50 ppm TNT after irradiation at 235 nm (Fig. 6). TNB is the only possible product that absorbs near this wavelength [26]. Fig. 7 shows SF spectra of 50 ppm TNT after reaction with Fenton reagent. Neither the dark Fenton free radical initiator, whose spectra is shown in Fig. 7, nor did irradiated Fenton reagent generate any TNT transformation.
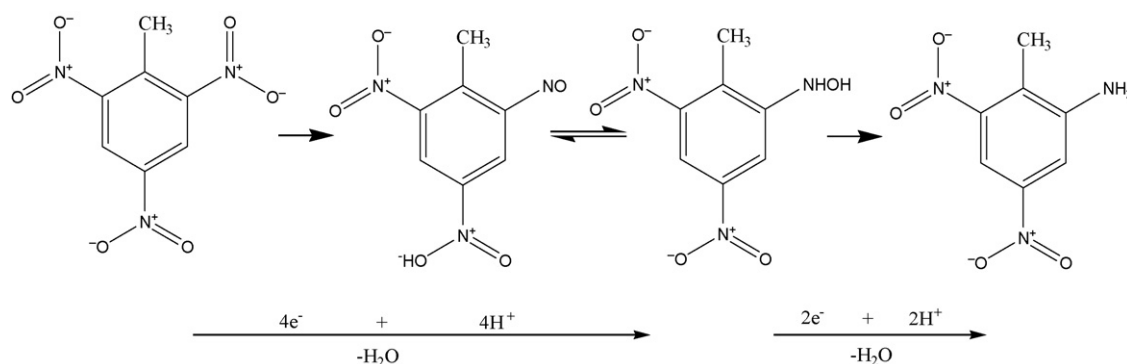

Fig. 4. TNT reductive transformations to nitroaromatic amines. The above pathway exemplifies the conversion of one of the nitro groups of TNT to an amino group in the presence of an acid.
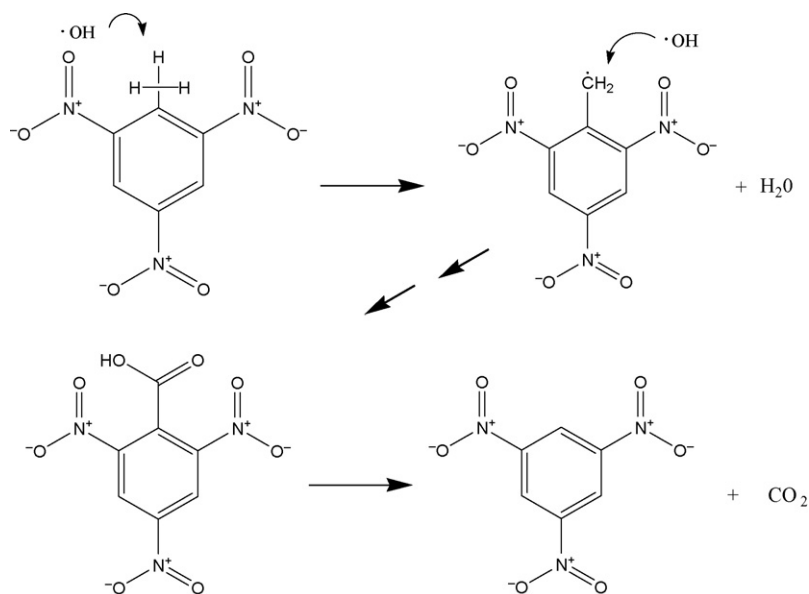
Fig. 5. Chemical oxidation of TNT by OH radical. Formation of 1,3,5-trinitro-benzene (TNB) is due to an oxidation mechanism, which is more light dependent than the reduction mechanism responsible for the formation of nitroaromatic amines.
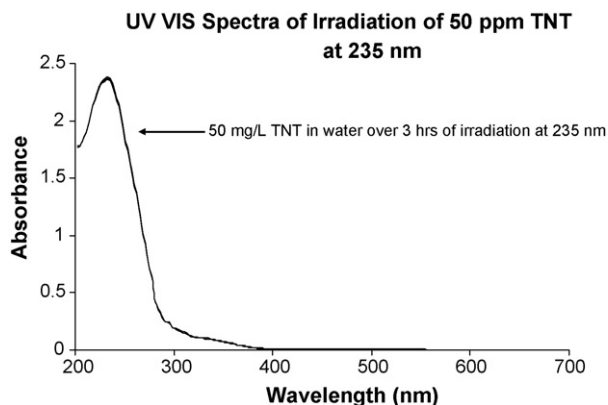

Fig. 6. UV Vis spectra of TNT after Irradiation at 235 nm. 50 ppm TNT was irradiated with light at 235 nm. UV Vis spectra were collected at intervals over a 24 h time period. No reaction occurs.

TNT, itself was not transformed through free radicals generated through either monochromatic irradiation or Fenton reagents. However, after alkaline hydrolysis, irradiation of the TNT products, TNB and TNP, which absorbed at 450 nm, was shown to be effective. UV Vis spectra of TNT irradiation at 235 nm of 50 ppm TNT and (A) 0.05N NaOH; (B) 0.5N NaOH; and (C) 1.0N NaOH is shown in Fig. 8 and is compared with Fig. 9 spectra of irradiation of the same concentrations at 450 nm. Spectral data suggested

that alkaline hydrolysis, by itself, of TNT, induced a decrease with time at the 235 nm peak in an irradiated system with all three concentrations of NaOH, even though photolysis, by itself, at the 235 nm wavelength of maximum absorption showed no significant change (Fig. 8). The 450 nm absorbance band (Fig. 9) also formed upon reaction of TNT and OH⁻. However, the intensity of this absorbance band decreased with time and eventually disappeared. At 0.05N NaOH concentration, both TNT and its intermediate peak persisted beyond 3 h. Little change can be expected at this low NaOH concentration since effective TNT transformation takes place at higher concentrations as seen with the 0.5N and 1.0N NaOH concentrations. This data suggests that the TNT analogues formed by NaOH remediation are susceptible to OH radical oxidative reactions at 450 nm. Alkaline hydrolysis of TNT, TNB and TNP form in the same absorption visible region (430–460 nm) suggesting a common intermediate with additional hydroxylation substituting for nitro groups and consequent loss of aromaticity—thus resulting in degradation of the parent compound [13,20,32].

5. Comparison of TNT analogues

In an attempt to discover relationships between structure, reactivity and toxicity, TNT and seventeen of its possible analogues were compared computationally, as seen in Table 1. Amino and hydroxyl groups were substituted at the 2,6- and 2,4-positions of the TNT molecule to produce the 17 analogues. In addition,
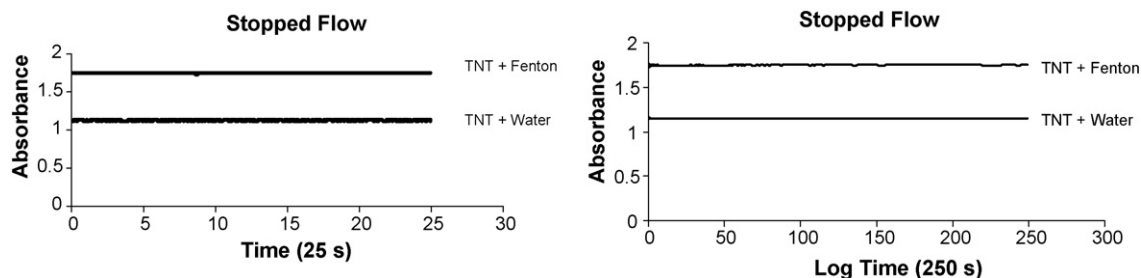

Fig. 7. Stopped flow of TNT after treatment with Fenton's reagent. 50 ppm TNT was treated with Fenton's reagent. SF spectra were immediately taken upon combination of the two solutions. No reaction occurs.
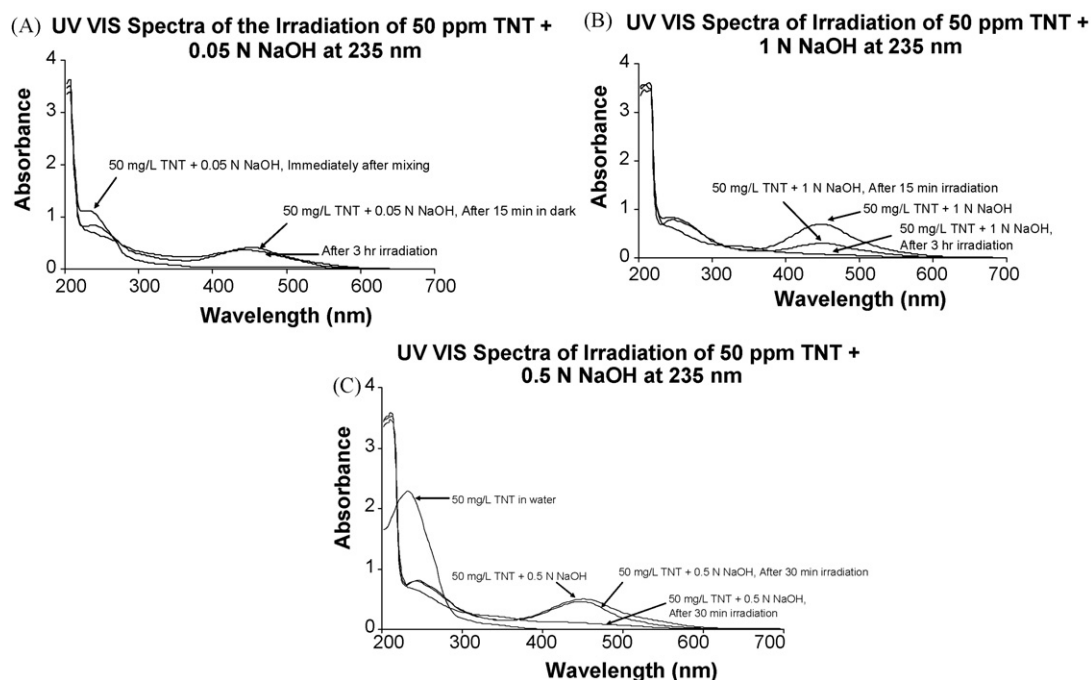
Fig. 8. UV Vis spectra of TNT after treatments with sodium hydroxide and irradiation at 235 nm. UV Vis spectra of 50 ppm TNT treated with (A) 0.05N NaO; (B) 0.5N NaOH; (C) 1N NaOH followed by irradiation at 235 nm were collected at intervals over a 24 h time period. Progression of product transformation was not affected by irradiation at 235 nm.

2,6- and 2,4-dinitrotoluenes were included in the comparison of dipole moments and of formation, steric, and HOMO/LUMO energies. Significant correlations relating structural changes to energy variations were obtained using both semiempirical and DFT computational approaches [19–20].

Data in Table 1 suggest that TNB has a slightly higher heat of formation and lower steric energy (MM2) than TNT due to inductive, steric, and electrostatic effects of the methyl group of TNT.

The same trend for heat of formation was obtained through DFT calculations where replacing the methyl group with an OH^- considerably lowered the heat of formation. For example, addition of OH^- to form picric acid (TNP) drives the heat of formation drastically lower than in either TNT or TNB. Compared to TNT and TNP, TNB has the highest heat of formation but the lowest steric, as well as the lowest HOMO/LUMO energies, as expected. The heat of formation decreased with higher concentrations of
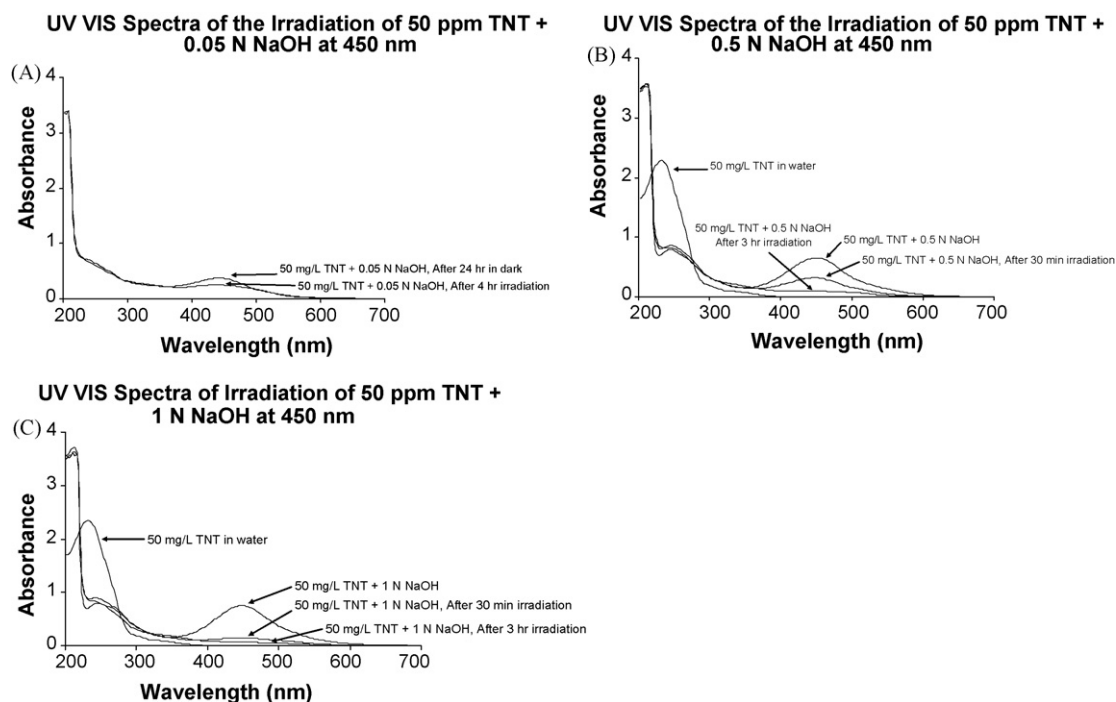

Fig. 9. UV Vis spectra of TNT after treatments with sodium hydroxide and irradiation at 450 nm. UV Vis spectra of 50 ppm TNT treated with (A) 0.05N NaOH; (B) 0.5N NaOH; (C) 1N NaOH followed by irradiation at 450 nm were collected at intervals over a 24 h time period. Irradiation speeded the transformation at 450 nm where product via alkaline hydrolysis appeared and disappeared.

OH^-. Also, heat of formation is consistent with HOMO/LUMO ratios [19–20].

In our research, AM1 and DFT B3LYP consistently showed that substituting an amine for the TNT nitro group results in the following: (i) HOMO energy values are always lower when the amine is substituted on the ortho C_2 rather than on the para C_4 position with respect to the methyl group, because amines add electrons to the aromatic ring, thereby activating them. This lowering of energy to the methyl group ortho position is due to both inductive and steric effects of the methyl group. (The resonance effect is the same for both ortho and para positions.). (ii) For both mono- and di-substituted amino and hydroxyl groups, HOMO and formation energies are always lowest when the substitution is on the ortho rather than the para position. For example, 2-amino is lower than 4-amino and 2-hydroxy is always lower than 4-hydroxy. (iii) The same trend pertains to diamino and dihydroxy substitutions on TNT. That is, 2,6-diamino and 2,6-dihydroxy are always lower than 2,4-diamino and 2,4-dihydroxy substitutions. (iv) The opposite effect is observed for the nitro groups due to their electron-withdrawing nature. For example, 2,6-dinitrotoluene has higher steric energy, heat of formation, and HOMO energy than 2,4-dinitrotoluene [19–20].

HOMO/LUMO energies increased while the heat of formation decreased with subsequent nitro group replacement by amino or hydroxyl groups. The greatest lowering of the heat of formation occurred with greatest hydroxyl group substitution. HOMO energy is lower when amines or hydroxyl groups are substituted at the ortho (2,6-) rather than the para (4-) position. This is true for both mono- and di-substitutions. For example, 2-amino and 2-hydroxyl positions are always of lower HOMO energy than 4-amino-dinitrotoluene and 4-hydroxyl-dinitrotoluene. Also 2,6-diamino-nitrotoluene and 2,6-hydroxyl-nitrotoluene are always of lower HOMO/LUMO energies than 2,4-dinitro-nitrotoluene and 2,4-dihyroxyl-nitrotoluene. On the other hand, due to the electron-withdrawing nitro groups, the trend is reversed in the dinitrotoluenes with the 2,4-dinitrotoluene always having lower HOMO/LUMO and formation energies than 2,6-dinitrotoluene [19–20].

Two factors that may affect toxicity positively and negatively: (i) Ortho are generally more toxic than para substituted amines; and ii) two adjacent hydroxyl groups or two hydroxyl groups para to each other may cause the aromatic parent compound to decompose into smaller molecules less toxic than the parent [13,19–20].

6. Summary and conclusion

In summary, TNT and selected derivatives were reacted with alkali hydrolysis in competing transformation mechanisms. They were also reacted with free radical initiators via monochromatic irradiation and via Fenton reactions. Effective TNT transformation intermediates and final products were produced, in our study, only by alkaline hydrolysis. However, after alkaline hydrolysis was carried out, monochromatic irradiation at 450 nm enhanced TNT transformation.

Pertaining to substituent influence as to structure and reactivity of TNT and its analogues: (i) Ortho are generally more toxic than para substituted amines; and (ii) two adjacent hydroxyl groups or two hydroxyl groups para to each other may cause the aromatic parent compound to decompose into smaller molecules less toxic than the parent [13,19–20].

Toxicity is one of the greatest and most obvious environmental concerns. The following conclusions pertain to the potential for toxic interactions of TNT and its derivatives and analogues in the environment. Pertaining to addition of OH^-: (i) It is a known fact that OH^- groups render molecules they are attached to more

water soluble, thereby facilitating metabolism [23–26]; (ii) under certain conditions, two adjacent OH^- can lose a water molecule and form a carcinogenic apoxy [25]. This principle applies to TNT and its derivatives, which can follow this pathway where, due to loss of a water molecule, OH^- can contribute to solubility and to the occasional formation of an apoxy; (iii) polymerization can cause creation of toxic compounds [32]. Azo dyes are formed through polymerization (dimerization) of nitrogen–carbon, carbon–carbon, or nitrogen–nitrogen bonds [32]. Therefore, in similar manner to azo dyes, known to be highly toxic, certain di-azo polymers of TNT can also be expected to be toxic.

In conclusion, semiempirical prediction and analysis coupled with UV Vis and SF spectroscopic corroboration provided a valid approach to our hypothesis that *molecular structure determines transformation pathways*. By reducing time and cost of predicting, identifying, screening, and prioritizing toxic transformations, theoretical calculation is both productive and proactive, particularly when substantiated as needed by spectroscopy. As computational methods, protocols, levels of complexity, and adaptability are continuously derived/improved, and as scope and accuracy of spectroscopic techniques advance, their combined application provides premier tools for predicting, characterizing, and analyzing transformation products of nitro energetics and other compounds of interest to the Department of Defense and chemical industries.

References

[1] M. Honeycutt, A. Jarvis, V. McFairland, Cytotoxicity and mutagenicity of 2,4,6-trinitrotoluene and its metabolites, Exotoxicol. Environ. Saf. 35 (1996) 282–287.
[2] Sciences International, Inc. (1995). Toxicological Profile for 2,4,6-Trinitrotoluene, U.S. Department of Health And Human Services, June 1995.
[3] D. Ownby, J. Belden, G. Lotufo, M. Lydy, Accumulation of trinitrotoluene (TNT) in aquatic organisms. Part I. Bioconcentration and distribution in channel catfish (*Ictalurus punctatus*), Chemosphere 58 (2005) 1153–1159;
D. Ownby, J. Belden, G. Lotufo, M. Lydy, Accumulation of trinitrotoluene (TNT) in aquatic organisms. Part II. Bioconcentration in aquatic invertebrates and potential for trophic transfer to channel catfish (*Ictalurus punctatus*), Chemosphere 58 (2005) 1161–1168.
[4] R. Bajpai, D. Parekh, S. Herrmann, M. Popovic, J. Paca, M. Qasim, A kinetic model of aqueous-phase alkali hydrolysis of 2,4,6-trinitrotoluene, J. Hazard. Mater. 106B (2004) 55–66.
[5] R. Bajpai, M. Qasim, L. Hansen, M. Popovic, J. Paco, Chemical and biological reactions of TNT and RDX, in: 15th International Congress of Chemical & Process Engineering, Chisa, Czech, 8/25-29/02, 2002.
[6] J. Brannon, M. Qasim, C. Price, S. Yost, Photodegradation of TNT in water & sediment/water systems, WES Rep. (peer reviewed), in: Env. Eng. Div.-USAE, WES, 1998.
[7] L. Hansen, S. Larson, D. Fell, M. Qasim, M. Cullinane, Base-catalyzed transformations of explosive compounds in soil & water, in: USACE Envirnment Development Workshop, 4/16/01, Portland, OR, 2001.
[8] Z. Li, P. Shea, S. Comfort, Destruction of 2,4,6-trinitrotoluene by Fenton oxidation, J. Environ. Qual. 26 (1997) 480–487.
[9] H. Christensen, et al., Reactions of hydroxyl radicals with hydrogen peroxide at ambient and elevated temperatures, J. Phys. Chem. 86 (9) (1982).
[10] L. Hundal, J. Singh, E. Bier, P. Shea, S. Comfort, W. Powers, Removal of TNT and RDX from water and soil using iron metal, Environ. Pollut. 97 (1997) 55–64.
[11] D. Schmelling, K. Gray, P. Kamat, Role of reduction in the photocatalytic degradation of TNT, Environ. Sci. Technol. 30 (1996) 2547–2555.

[12] L. Krumholz, J. Li, W. Clarkson, G. Wilber, J. Suflita, Transformations of TNT and related aminotoluenes in groundwater aquifer slurries under different electron-accepting conditions, J. Indus. Microbiol. Biotechnol. 18 (2–3) (1997) 161–169.

[13] M. Qasim, R. Bajpai, L. Hansen, Nucleophilic reactions of TNT with OH-" for enhancement of biodegradation, in: Oral: 4th International Conference, TiO$_2$ Photocatalytic Purification & Treatment of Water & Air, Part of: 5th International Conference on Advanced Oxidation Technologies for Water & Air Remediation, Albuquerque, NM, 5/99, 1999.

[14] E. Davis, R. Boopathy, J. Manning, Use of trinitrobenzene as a nitrogen source by *Pseudomonas vesicularis* isolated from soil, Curr. Microbiol. 34 (3) (1997) 192–197.

[15] R. Boopathy, J. Manning, Surfactant-enhanced bioremediation of soil contaminated with 2,4,6-trinitrotoluene in soil slurry reactors, Water Environ. Res. 71 (1999) 19–24.

[16] C. Vorbeck, H. Lenke, P. Fischer, H. Knackmuss, Identification of a hydride-meisenheimer complex as a metabolite of 2,4,6-trinitrotoluene by a *Mycobacterium* strain, J. Bacteriol. (February) (1994) 932–934.

[17] M. Qasim, R. Bajpai, M.A. Majors, Enhancing TNT biodegradability by chemical transformation of TNT, in: SERDP 4th TAC Meeting, Washington, DC, 6/98, 1998.

[18] P. Politzer, J. Murray, J. Seminario, P. Lane, M. Grice, M. Concha, Computational characterization of Energetic materials, J. Mol. Struct. (Theochem.) 573 (2001) 1–10.

[19] M. Qasim, P. Honea, H. Fredrickson, J. Furey, A comparative study of energies and other properties of TNT and related compounds, in: 5th Southern School of Computational Chemistry, Jackson, MS 4/8-9/05, 2005.

[20] M. Qasim, P. Honea, H. Fredrickson, Comparative study of reaction mechanisms of TNT and selected analogues using free radical generators and alkaline: hydrolysis, in: 2nd DoD Sustainable Ranges Initiative, San Antonio, TX, 8/22-25/05, 2005.

[23] F. Carey, Organic Chemistry, 418–24, McGraw-Hill, New York, 1987, pp. 448–461.

[24] S. Ege, Organic Chemistry, Heath and Co, Lexington, MA, 1989.

[25] M. March, *Advanced Organic* Chemistry: Reactions, Mechanisms and Structure, 4th ed., Wiley, 1992, p. 652.

[26] A. Streitwieser, C. Heathcock, E. Kosower, Introduction to Organic Chemistry, NYC, Macmillan, 1992.

[27] S. Patai (Ed.), Supplement F2: The Chemistry of Amino, Nitroso, Nitro and Related Groups Part 1, John Wiley, Chichester, 1996.

[28] L. Gorb, A. Blue, J. Leszczynski, The interactions of the aromatic nitrocompounds with the surface of hydrated clay minerals. An ab initio study, in: 7th Conference on Current Trends in Computational Chemistry, Vicksburg, MS, 11/6-7/98, 1998.

[29] R. Lutchyn, Y. Zub, L. Gorb, J. Leszczynski, Molecular models of 1,3,5-trinitrobenzene. An ab initio quantum chemical study, in: 9th Conference on Current Trends in Computational Chemistry, Vicksburg, MS, 11/3-4/2000, 2000.

[30] A. Nielsen, Nitrocarbons, Organic Chemistry Series, VCH Publ., Inc., 1995.

[31] S. Haderlein, T. Hofstetter, R. Schwarzenbach, Surface chemistry of nitroaromatic compounds, in: J.C. Spain, J.B. Hughes, H.-J. Knackmuss (Eds.), Biodegradation of Nitroaromatic Compounds And Explosives, CRC Press, Boca Raton, FL, 2000, Chapter 12.

[32] K. Thorn, P. Thorne, L. Cox, Alkaline hydrolysis/polymerization of 2,4,6-trinitrotoluene: characterization of products by ^{13}C and ^{15}N NMR, Environ. Sci. Technol. 38 (2004) 2224–2231.

[33] M. Qasim, Y. Kholod, L. Gorb, D. Magers, P. Honea, J. Leszyznski, Application of quantum–chemical approximations to environmental problems: prediction of physical and chemical properties of TNT and related species, Chemosphere 69 (2007) 1144–1150.

Further reading

[21] J. Stewart, MOPAC 2000 Manual, Fujitsu Limited, 1999.

[22] W. Caper, E. Davis, M. Extine, Molecular structure of 2,3,6-trinitrotoluene, J. Phys. Chem. (1982) 86.